Supplement of Atmos. Chem. Phys., 16, 2611–2629, 2016
http://www.atmos-chem-phys.net/16/2611/2016/
doi:10.5194/acp-16-2611-2016-supplement

Atmospheric Chemistry and Physics Open Access EGU

Supplement of

Understanding cirrus ice crystal number variability for different heterogeneous ice nucleation spectra

Sylvia C. Sullivan et al.

Correspondence to: Athanasios Nenes (athanasios.nenes@gatech.edu)

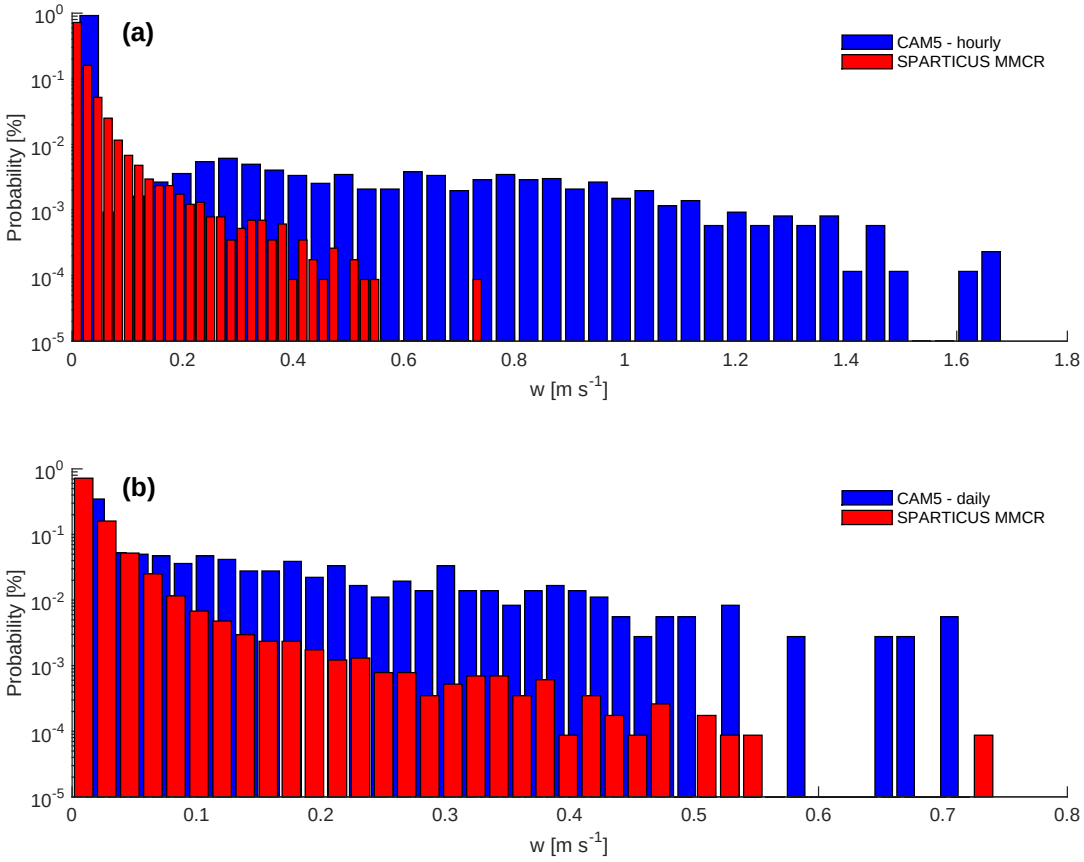

Figure S1. Comparison of the distribution of model input updraft velocities and of millimeter cloud radar (MMCR)-measured updraft velocities after Doppler velocity decomposition. Data include all hourly averaged values from the ARM SGP site (36.605°N, 97.485°W) throughout 1997 at the 230 ± 20 hPa pressure levels (www.arm.gov/data/pi/76). These are compared to **(a)** hourly averaged updrafts at 232 hPa from a year-long CAM 5.1 simulation at the same latitude and longitude and **(b)** the daily averaged updrafts over those hourly values in **(a)**. Daily averaged values agree better with the observed updraft velocities and are used to run all simulations. A strong filter for convective towers has been applied to the data and may explain its lack of higher values.

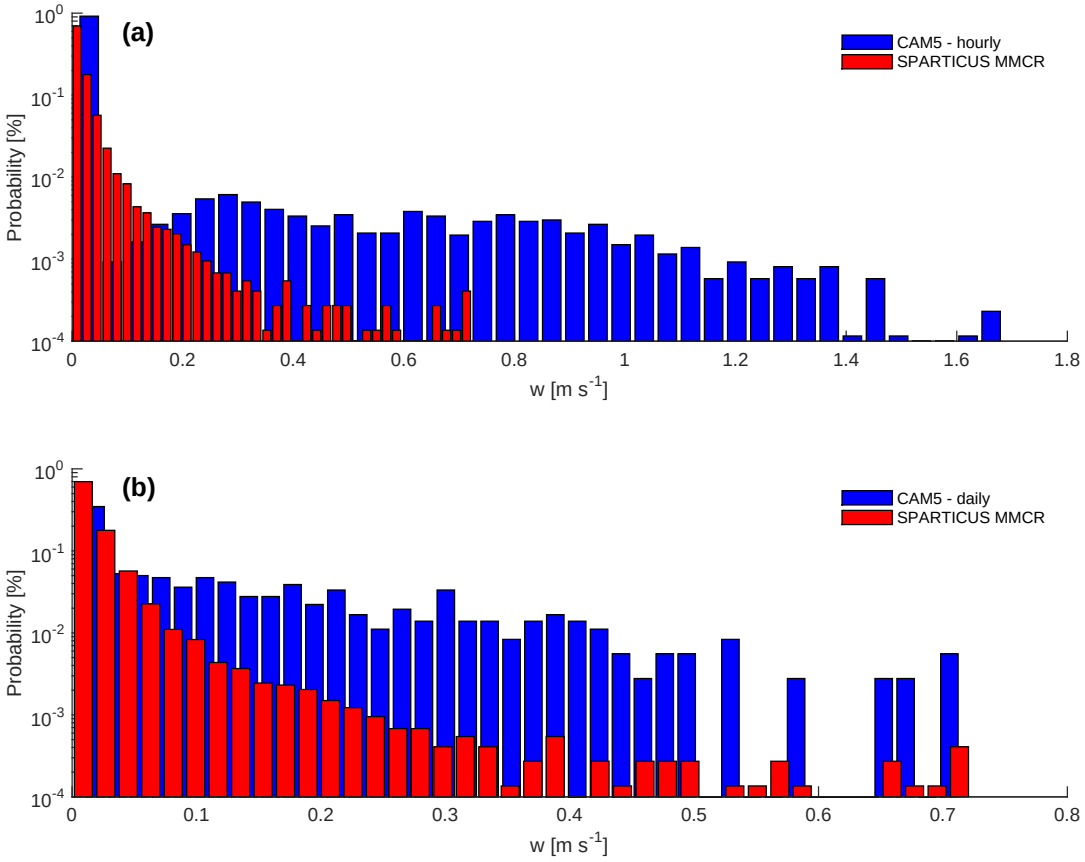

Figure S2. Comparison of the distribution of model input updraft velocities and of millimeter cloud radar (MMCR)-measured updraft velocities after Doppler velocity decomposition. Data include all hourly averaged values from the ARM SGP site (36.605°N, 97.485°W) throughout 2007 around the 230 $\pm$ 20 hPa pressure levels (www.arm.gov/data/pi/76). These are compared to **(a)** hourly averaged updrafts at 232 hPa from a year-long CAM 5.1 simulation at the same latitude and longitude and **(b)** the daily averaged updrafts over those hourly values in **(a)**. Daily averaged values agree contain fewer instances of very large updraft and are used to run all simulations. A strong filter for convective towers has been applied to the data and may explain its lack of higher values.

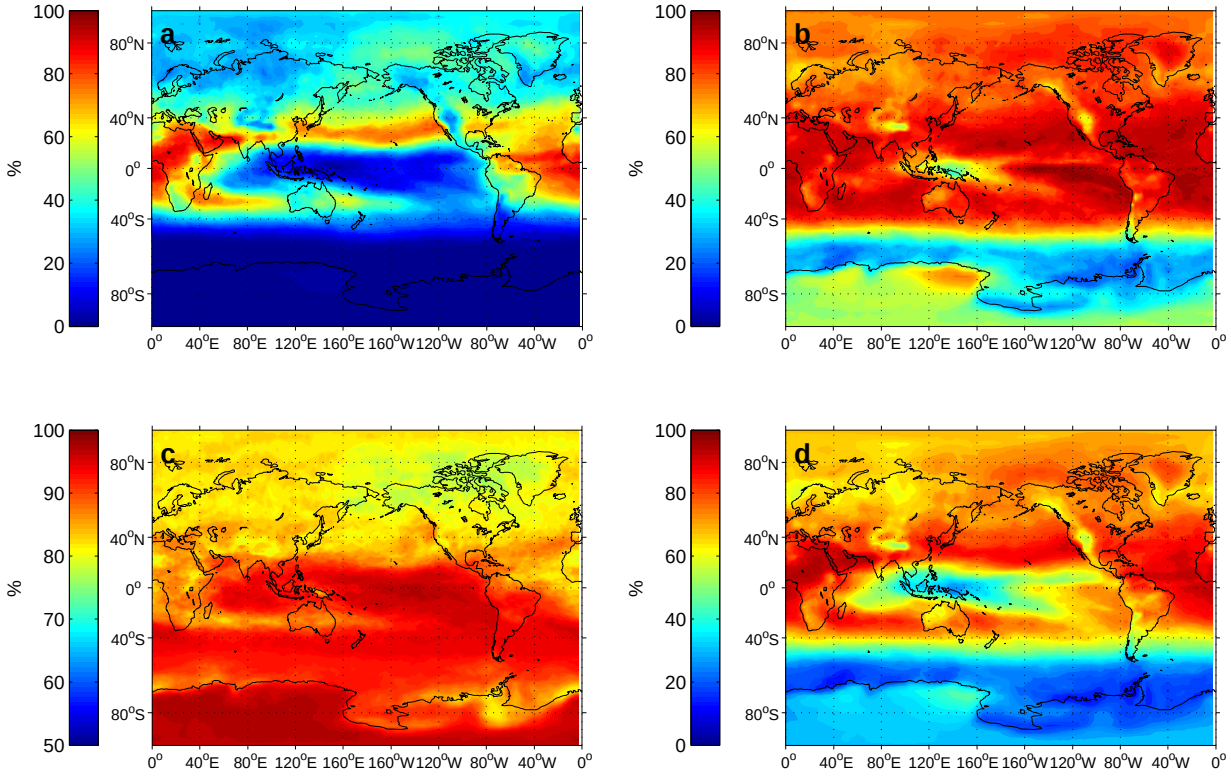

Figure S3. Annually averaged heterogeneously formed fraction for **(a)** PDA08, **(b)** PDA13, **(c)** CNT, and **(d)** AIDA nucleation spectra. The colorbar for panel **(c)** is different than the others.

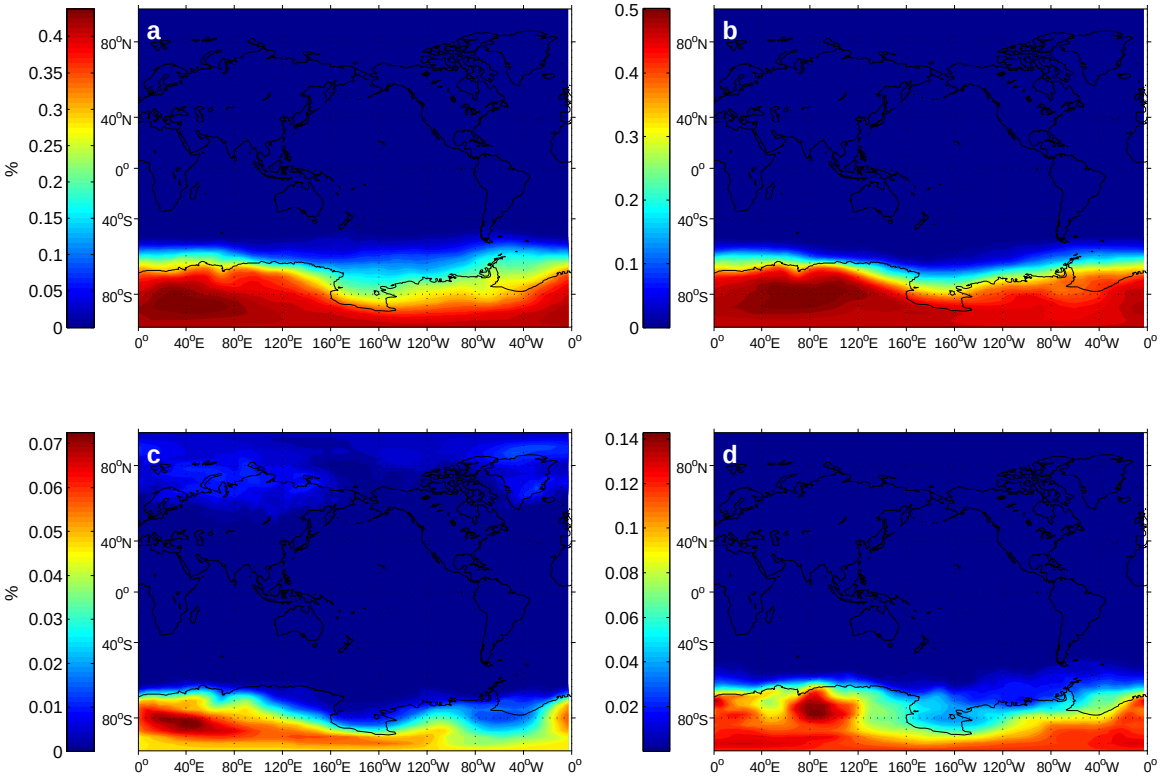

Figure S4. Glassy soluble organic aerosol contribution to heterogeneously formed crystal number in PDA13 for **(a)** June, July, August; **(b)** September, October, November; **(c)** December, January, February; and **(d)** March, April, and May.

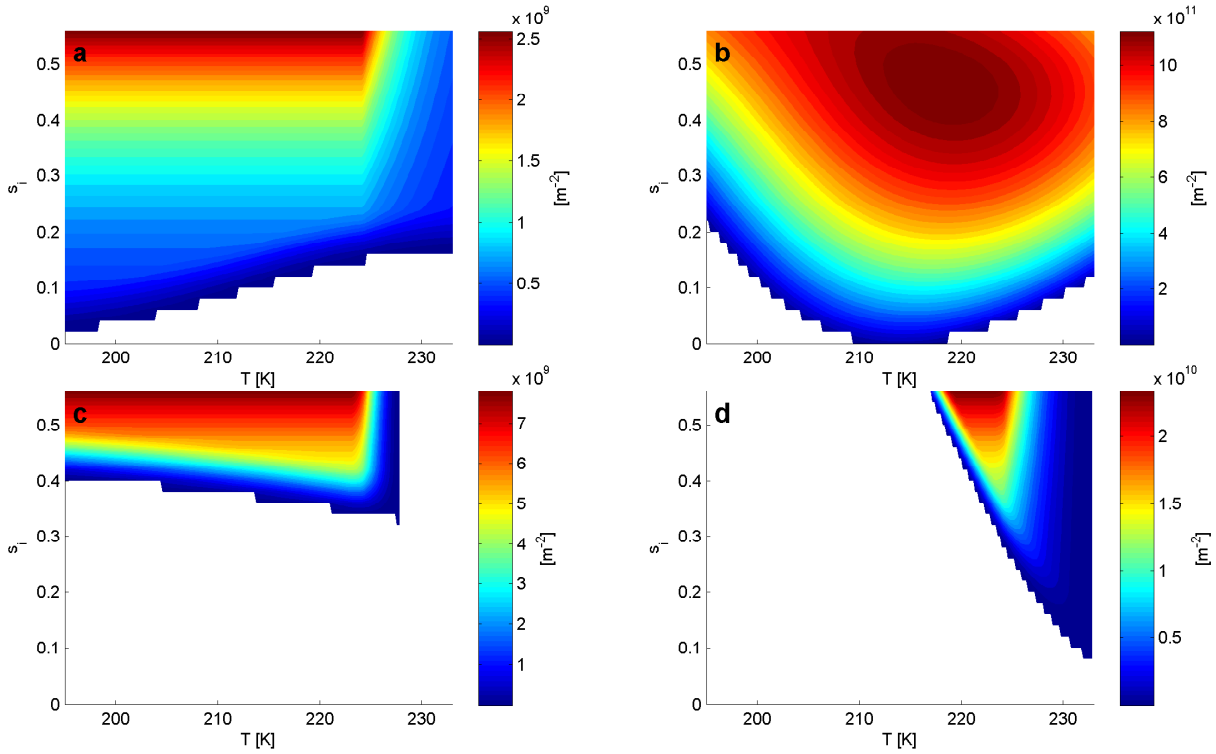

Figure S5. Active site densities in the temperature-supersaturation space for **(a)** dust in PDA08 and PDA13, **(b)** dust in AIDA, **(c)** BC in PDA08, and **(d)** BC in PDA13.